ISSN 0023-1584, Kinetics and Catalysis, 2015, Vol. 56, No. 3, pp. 308–315. © Pleiades Publishing, Ltd., 2015.
Original Russian Text © Li Na, A.V. Vorontsov, Jing Liqiang, 2015, published in Kinetika i Kataliz, 2015, Vol. 56, No. 3, pp. 310–317.

Physicochemical Properties and Photocatalytic Activity of $H_3PW_{12}O_{40}/TiO_2$

Li Na[a, b], A. V. Vorontsov[a, *], and Jing Liqiang[b, **]

[a] *Boreskov Institute of Catalysis, Siberian Branch, Russian Academy of Sciences, Novosibirsk, 630090 Russia*

[b] *Heilongjiang University, Harbin, China*

**e-mail: a-voronts@yandex.ru*

***e-mail: jinglq@hlju.edu.cn*

Received September 11, 2014

Abstract—For enhancing its photocatalytic activity, titanium dioxide P25 has been modified by adsorption of the heteropoly acid (HPA) $H_3PW_{12}O_{40}$ from aqueous solution at an HPA concentration of 0.2 to 5 mmol/L. The deposition of the HPA does not alter the phase composition or morphology of the photocatalyst but only causes a slight change in its diffuse reflectance spectrum. IR spectroscopic and XPS studies have confirmed that the HPA molecules on the TiO_2 surface are intact. The adsorption of the HPA increases the photovoltage and hydroxyl radical yield under UV irradiation. These characteristics reach their maximum values upon the adsorption of the HPA from its 0.5 mmol/L solution. Electrochemical measurements have demonstrated that the HPA increases the rate of interfacial electron transfer. The deposition of the HPA accelerates the gas-phase oxidation of acetaldehyde and the degradation of phenol and triethyl phosphate in the aqueous medium. The highest activity is shown by the catalyst obtained by the adsorption of $H_3PW_{12}O_{40}$ from its 0.5 mM solution. The results of this study suggest that the HPA is promising for modifying the surface of the TiO_2 photocatalyst.

DOI: 10.1134/S0023158415030131

Photocatalytic oxidation converts organics into inorganic compounds in aqueous media [1–5] and in air [6, 7]. This process, also called mineralization, is applicable to water and air purification [8, 9]. The photocatalytic oxidation of impurities in aqueous solution may be accompanied by the evolution of hydrogen, a valuable fuel and raw material [10–13].

The most common deep oxidation catalyst is titanium dioxide, which is an inexpensive, stable, and nontoxic material [14, 15]. However, TiO_2 suffers from a serious drawback: its photocatalytic activity is insufficiently high [16]. One way of enhancing its activity under UV irradiation is by introducing a surface modifier, such as titanium dioxide, which favors the separation of photogenerated charges [17, 18], increases the electron transfer rate [19], and enhances light absorption [20, 21] and the adsorption of oxygen [22] and contaminants from water and air [23]. In addition, it is favorable for the occurrence of some dark steps of degradation.

Heteropoly acids (HPAs) have rather long been used as dark step catalysts [24–26] and photocatalysts [27–31]. The highest activity in photocatalytic oxidation reactions is shown by $H_3PW_{12}O_{40}$ [32–34]. Serving as acid and redox catalysts, HPAs accelerate numerous organic synthesis reactions [35–37].

It was not until recently that HPAs found use as surface modifiers for titanium dioxide intended for photocatalytic applications [38]. Their role in photochemical processes has largely been limited to separation of photogenerated charges via the reduction of their adsorbed molecules.

There are two methods of preparing HPA/TiO_2 composites. In the first method, an HPA is introduced at some TiO_2 synthesis stage [39, 40]; in the second, an HPA as a colloid, suspension, or film is adsorbed onto off-the-shelf titanium dioxide [38, 41]. HPAs were anchored to a TiO_2 film by heat-treating the latter at 300°C [42], 350°C [43], and 400°C [44]. In all cases, HPA deposition accelerated the photochemical oxidation reaction.

In this study, we used the simplest possible method of preparing the $H_3PW_{12}O_{40}/TiO_2$ catalyst: the HPA was adsorbed onto titanium dioxide P25 in aqueous suspension without subsequently heat-treating the product. The resulting photocatalysts were comprehensively characterized, and their photocatalytic activity was measured in acetaldehyde oxidation in the vapor phase and in phenol and triethyl phosphate oxidations in solution. The highest activity in the mineralization of these compounds was observed for catalysts containing small amounts of deposited HPA.

EXPERIMENTAL

Chemicals

The chemicals used in this study were TiO_2 Degussa P25, analytical-grade $H_3PW_{12}O_{40}$ (Tianjin Guangfu Fine Chemical Research Institute), analyti-

cal-grade HNO_3 (AR, Sinopharm), air containing 997.2 ppm acetaldehyde (Dalian Special Gases Co.), analytical grade phenol (AR, Tianjin Kemiou Chemical Reagent Development Center), and >99.8% triethyl phosphate (Sigma-Aldrich). All chemical were used as received. Experiments were carried out using distilled or additionally purified water.

Photocatalyst Preparation

The $H_3PW_{12}O_{40}/TiO_2$ photocatalysts were prepared by HPA adsorption from aqueous solution. To prevent the HPA from decomposition, it was dissolved in a 0.1 M aqueous HNO_3 solution with pH 1. Solutions containing 0, 0.2, 0.5, 1.0, and 5.0 mmol/L of $H_3PW_{12}O_{40}$ were prepared. A 50-mL portion of a solution was poured into a beaker containing 0.5 g of a TiO_2 powder. The suspension was stirred at room temperature for 2 h, and the photocatalyst was then isolated by centrifugation. The resulting solid was washed with deionized water, centrifuged, dried in a vacuum at 80°C for 4 h, and then ground. The $TiO_2/H_3PW_{12}O_{40}$ samples prepared in this way were white. Hereafter, the samples prepared by adsorption from 0, 0.2, 0.5, 1.0, and 5.0 mM HPA solutions are designated T, 0.2P-T, 0.5P-T, 1.0P-T, and 5.0P-T, respectively.

Catalyst Characterization

Phase composition and crystallite size were estimated using a D/max-RB X-ray diffractometer (Rigaku, Japan).

The morphology of catalysts was studied by transmission electron microscopy (TEM) on a JEOL JEM-2010 microscope (Japan).

For measuring photocatalytic activity in the liquid phase and for obtaining the diffuse reflectance spectra (DRS) of photocatalysts, we used a UV-2550 UV–Vis spectrophotometer (Shimadzu, Japan).

The catalysts were also characterized by IR Fourier-transform spectroscopy on a Spectrum One spectrometer (PerkinElmer, United States).

The X-ray photoelectron spectroscopic (XPS) characterization of the catalysts was carried out using an ESCALABMKII spectrometer (VG, United Kingdom).

The efficiency of separation of photoinduced charges and the photoelectric properties of the catalysts were estimated by surface photo-emf spectroscopy (SPS) using an instrument fabricated at Heilongjiang University [18, 45].

Steady-state surface photovoltage spectroscopy was also carried out using a homemade device fitted with an SR830 lock-in amplifier synchronized with an SR540 optical chopper. A powder sample was fixed between two ITO glass electrodes in a controlled-atmosphere container having a quartz window. Monochromatic light was obtained by passing the radiation from a 500-W xenon lamp (CHF XQ500W) through an SBP300 monochromator.

Photocatalytic Activity Measurements

The activity of catalysts was measured in the photocatalytic oxidation of acetaldehyde vapor in the gas phase and in the photocatalytic oxidation of phenol and triethyl phosphate in an aqueous medium. The gas-phase reaction was conducted in a 0.5-L cylindrical quartz reactor into which an oxygen-diluted acetaldehyde–air mixture at an initial acetaldehyde concentration of 810 ppm was introduced. A photocatalyst sample (0.1 g) was placed onto the reactor bottom (6 cm^2) and was irradiated for 1 h with a 9-W UV lamp (Qiaolin Guang Electric Co., Shenzhen City) with an emittance maximum at $\lambda_{max} = 365$ nm. The acetaldehyde concentration in the reactor was measured using a GC-2014 gas chromatograph (Shimadzu, Japan) fitted with a flame-ionization detector.

In photocatalytic oxidation of phenol, 0.1 g of a photocatalyst was added to 100 mL of a solution with a phenol concentration of 10 mg/L. The experiments were carried out in a 100-mL glass reactor irradiated with light from a 150-W xenon lamp placed at a distance of about 10 cm from the reactor. The irradiation time was 1 h. During the reaction, 10-mL samples were withdrawn from the reactor and centrifuged, and 4-aminoantipyrine was then added to the samples. The phenol concentration was determined photometrically at a wavelength of 510 nm.

Photocatalytic oxidation of triethyl phosphate was carried in an aqueous suspension of the photocatalyst (150 mL). The initial triethyl phosphate concentration was 0.4 mmol/L, and the photocatalyst concentration was 0.5 mg/mL. The suspension was irradiated with a 18-W Dulux L lamp (Osram) placed just over the beaker with the reaction mixture. During the reaction, 0.8-mL samples were taken from the reactor, which were then filtered through a 0.2-μm filter and were analyzed on an anion-exchange column of a Model 861 ion chromatograph (Metrohm, Switzerland).

RESULTS AND DISCUSSION

Properties of Photocatalysts

Figure 1 shows the X-ray diffraction patterns of photocatalyst sample differing in the amount of $H_3PW_{12}O_{40}$ deposited. The characteristic peaks occur at $2\theta = 25.16°$, 37.8°, 48.05°, 53.9°, 55.06°, and 62.7°. According to the JCPDS 21-1272 card [46], they are, respectively, the (101), (004), (200), (105), (211), and (204) reflections from anatase. The characteristic peaks of rutile occur at $2\theta = 27.54°$, 36.06°, and 54.28°, according to JCPDS 65-0190 [47, 48]. The crystallite size for all samples was calculated via the Scherrer formula to be approximately 19.7 nm [40]. As is clear from Fig. 1, the introduction of phosphotung-

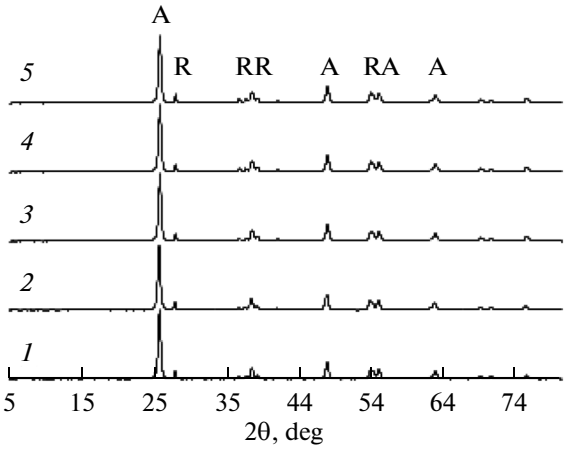

Fig. 1. X-ray diffraction patterns of titanium dioxide samples modified with $H_3PW_{12}O_{40}$ at its different concentrations: (*1*) TiO_2, (*2*) 0.2P-T, (*3*) 0.5P-T, (*4*) 1.0P-T, and (*5*) 5.0P-T.

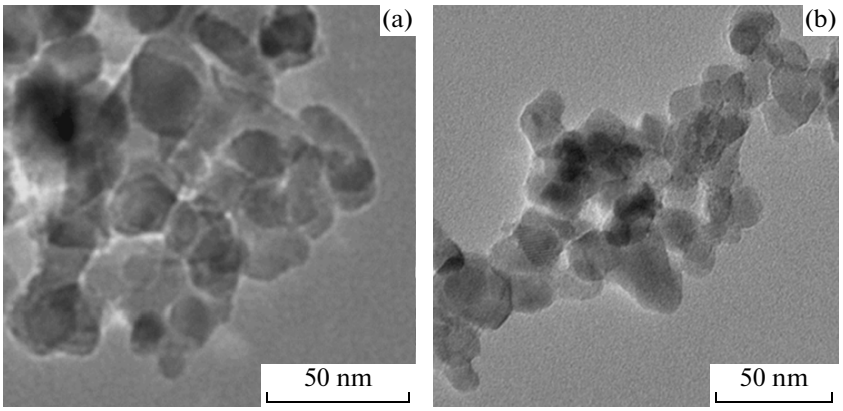

Fig. 2. TEM images of the (a) T and (b) 0.5P-T samples.

stic acid does not generate new phases and does not change the phase composition of the TiO_2 P25 powder. No diffraction peaks from $H_3PW_{12}O_{40}$ were observed even at the highest HPA concentration. This may be evidence that the acid on the TiO_2 surface is finely divided and does not form crystallites.

Figure 2 presents TEM images of individual titanium dioxide and one of the $H_3PW_{12}O_{40}/TiO_2$ photocatalysts. It can be seen that TiO_2 and titanium dioxide modified with $H_3PW_{12}O_{40}$ at a concentration of 0.5 mmol/L have the same morphology. The particles in both samples have the same roundish shape and the same size, namely, 20–40 nm. No obvious changes were revealed on the surface of modified TiO_2. This is further evidence of a uniform HPA distribution on the surface.

The diffuse reflectance spectra of the photocatalysts modified with different amounts of $H_3PW_{12}O_{40}$ are shown in Fig. 3. Light absorption by individual titanium dioxide starts at $\lambda < 420$ nm, which corresponds to a band gap width of about 3 eV, which is characteristic of anatase and rutile. The spectrum of $H_3PW_{12}O_{40}$ shows absorption peaks near 190 and 260 nm, so the HPA does not affect the diffuse reflectance spectrum of TiO_2, its spectrum being merged with the intrinsic absorption band of this semiconductor. Light reflectance in the 500–700 nm range decreases slightly as a result of HPA deposition. This may be due to the generation of defects, such as Ti^{3+} ions.

The IR spectroscopic data for TiO_2 samples modified with $H_3PW_{12}O_{40}$ at different concentrations are presented in Fig. 4. The spectra show distinct absorption bands at 966, 1074, 1385, 1461, and 1630 cm^{-1}. The bands at 1385 and 1630 cm^{-1} in the spectrum of individual titanium dioxide are due to carbonates and bending vibrations of hydroxyl groups and water molecules. The spectrum of $H_3PW_{12}O_{40}$ contains four characteristic absorption bands at 822, 893, 982, and

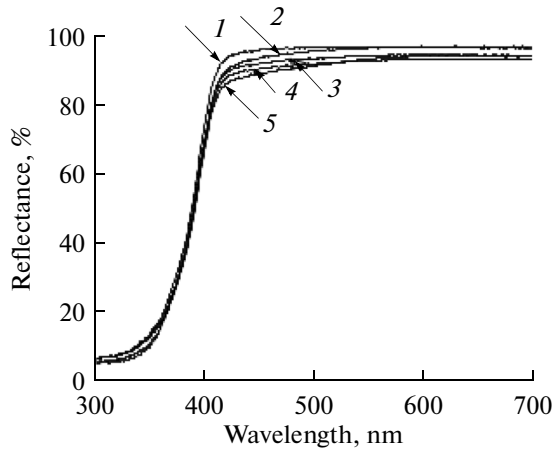

Fig. 3. Diffuse reflectance spectra of photocatalysts: (*1*) T, (*2*) 0.2P-T, (*3*) 0.5P-T, (*4*) 1.0P-T, and (*5*) 5.0P-T.

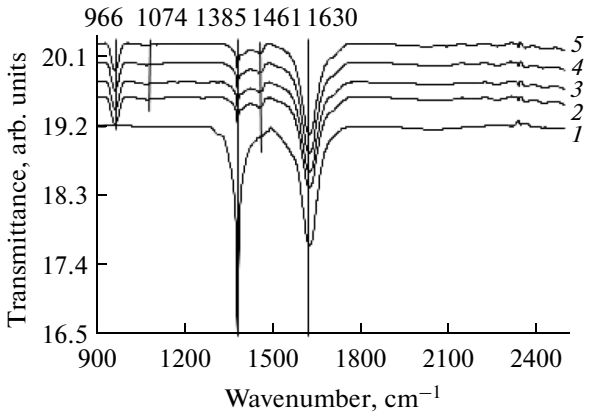

Fig. 4. IR spectra of photocatalysts: (*1*) T, (*2*) 0.2P-T, (*3*) 0.5P-T, (*4*) 1.0P-T, and (*5*) 5.0P-T.

1080 cm^{-1}. The bands at 822 and 893 cm^{-1} are merged with the strong absorption band of the anatase lattice (not shown in Fig. 4). The 1074 cm−1 band arises from P–O stretching vibrations; the 966 cm^{-1} band, from W=O stretching vibrations [44]. Thus, the Keggin structure of the HPA persists after the deposition of the acid onto the titanium dioxide surface. The absorption band at 1461 cm^{-1} is assignable to vibrations of the Ti–Cl bond.

The elemental composition of the photocatalyst surface and the valence state of elements therein were studied by XPS. The Ti2$p_{3/2}$ and Ti2$p_{1/2}$ lines of titanium dioxide (Fig. 5) occur at 458.4 and 464.9 eV [10], and the O1*s* band occurs at 529.5 eV [11]. It is clear from Fig. 5 that $H_3PW_{12}O_{40}$ deposition shifts the O1*s* line to higher energies, which may be due to the contribution from HPA oxygen, which shows itself at a binding energy of about 531.5 eV [12]. The characteristic W4*f* peaks appear at 35.8 eV (7/2) and 37.8 eV (5/2) [13]. A weak P2*p* peak is observed at 133.6 eV and is due to P^{5+}.

Figure 6 shows how the weight of individual TiO_2 and that of TiO_2 modified with $H_3PW_{12}O_{40}$ change during heating to 1000°C. Up to 120°C, the samples lose physically adsorbed water. As the temperature is further raised to 600°C, titanium dioxide and the $H_3PW_{12}O_{40}/TiO_2$ composite lose chemically bound water. Above 600°C, a marked weight loss (6 wt %) is observed for the 5.0P-T sample, which is due to the decomposition of adsorbed $H_3PW_{12}O_{40}$.

Thus, the examination of the $H_3PW_{12}O_{40}/TiO_2$ photocatalyst demonstrated that the HPA deposited on titanium dioxide is intact and is uniformly distributed on the surface.

The SPS method is used to study the separation of photogenerated charges [14, 15]. Figure 7 shows the photo-emf spectra of all of the catalysts considered. As the HPA content is increased, the photovoltage initially increases and then decreases, passing through a maximum in the case of 0.5P-T. Therefore, the introduction of a moderate amount of $H_3PW_{12}O_{40}$ is favorable for the separation of photoinduced charges. The decrease in photovoltage at high $H_3PW_{12}O_{40}$ contents can be explained by the absorption of part of the UV radiation by the HPA and by the changes in the properties of the adsorbed HPA as a consequence of its aggregation.

The hydroxyl radical $^{\cdot}OH$ is considered to be a key active species initiating photocatalytic oxidation. A widespread high-sensitivity method of detecting this radical is coumarin fluorescence [16]. The intensity of fluorescence from coumarin is proportional to the number of hydroxyl radicals with which it reacts. Figure 8 presents the luminescence spectra of coumarin recorded after the 1-h-long irradiation of the catalysts. It can be seen that the amount of hydroxyl radicals in the case of $H_3PW_{12}O_{40}/TiO_2$ is larger than in the case of individual titanium dioxide. The amount of hydroxyl radicals decreases upon the deposition of 0.5 mmol/L of $H_3PW_{12}O_{40}$. Thus, the 0.5P-T photocatalyst is characterized by the highest photo-emf and generates the largest number of hydroxyl radicals.

The addition of an HPA not only favors the separation of photogenerated charge carriers and increases the hydroxyl radical yield but can also increase the rate of interfacial electron transfer [20]. To verify this point, we recorded current–voltage curves for titanium dioxide suspensions containing different $H_3PW_{12}O_{40}$ concentrations (Fig. 9). As can be seen, the addition of the HPA increases the current density, which reaches its maximum at an $H_3PW_{12}O_{40}$ concentration of 5×10^{-6} mol/L. The introduction of a higher HPA concentration diminishes the current density. Therefore, the HPA increases the rate of electron transfer from the electrode material to the solution as well, since $H_3PW_{12}O_{40}$ is more readily reducible than water protons.

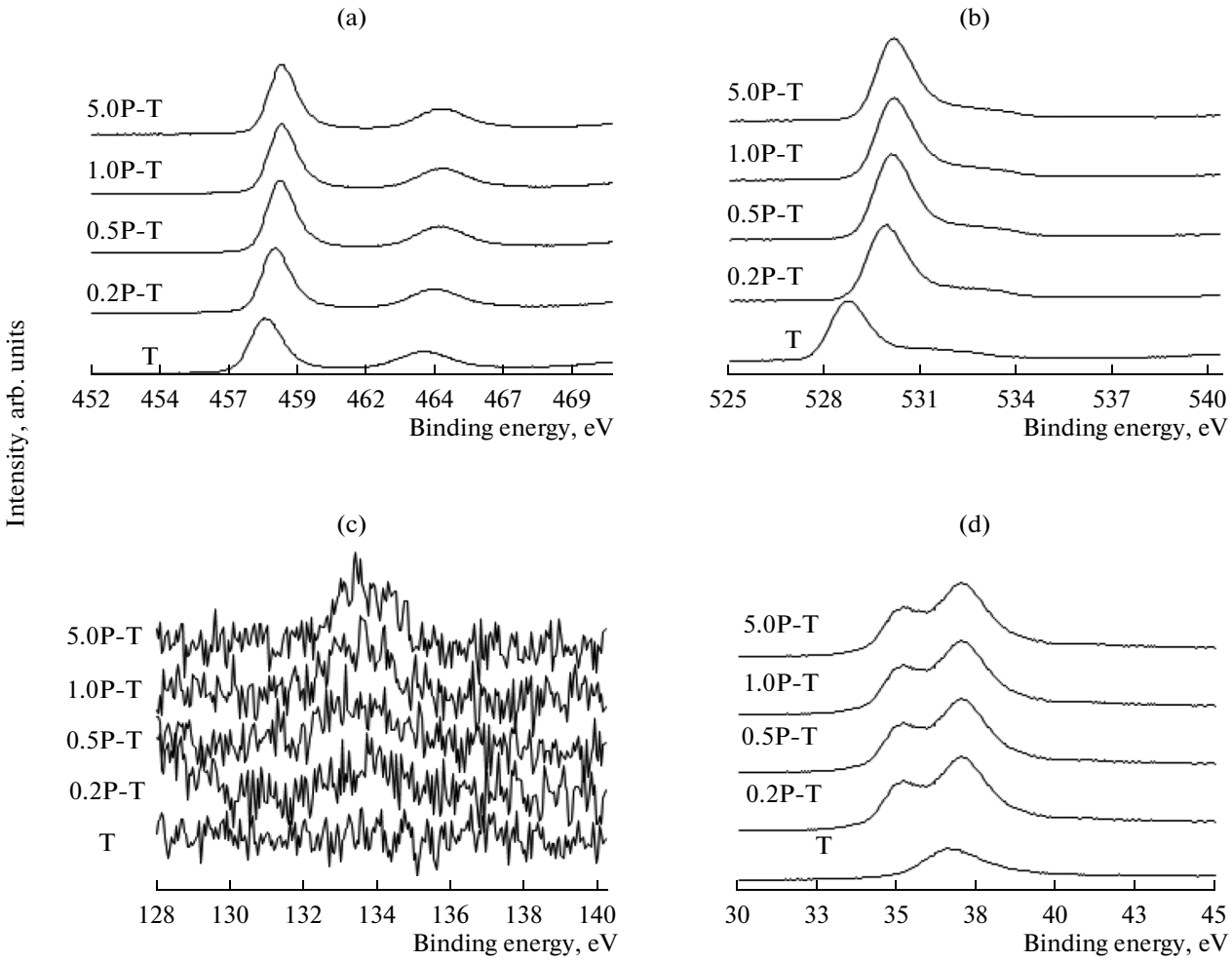

Fig. 5. X-ray photoelectron spectra of photocatalysts: (a) Ti2*p*, (b) O1*s*, (c) P2*p*, and (d) W4*f*.

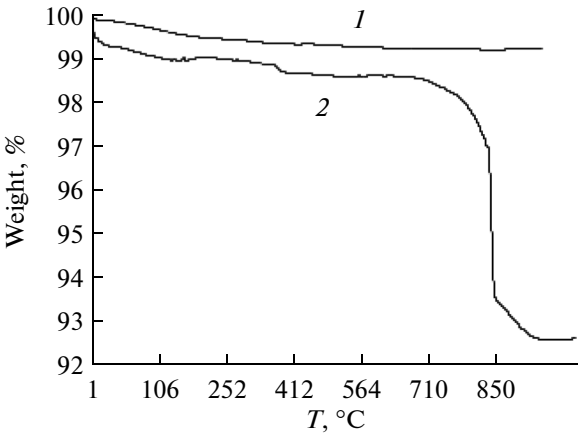

Fig. 6. Thermogravimetric profiles for the (*1*) T and (*2*) 5.0P-T samples.

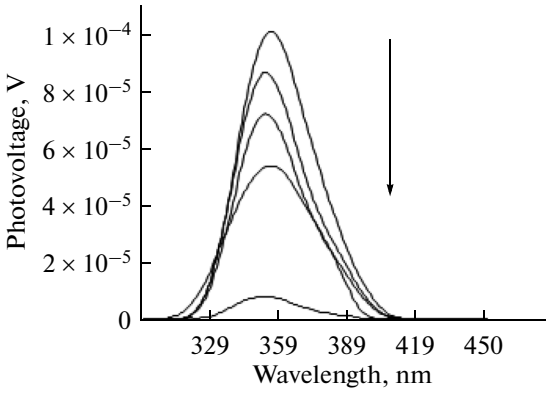

Fig. 7. Photo-emf spectra of photocatalysts. From top down: 0.5P-T, 0.2P-T, 1.0P-T, 5.0P-T, and T.

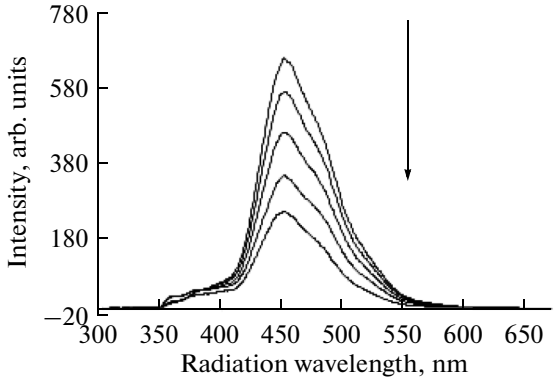

Fig. 8. Luminescence spectra of coumarin after the 1-h-long UV irradiation of photocatalyst samples. From the top down: 0.5P-T, 0.2P-T, 1.0P-T, 5.0P-T, and T.

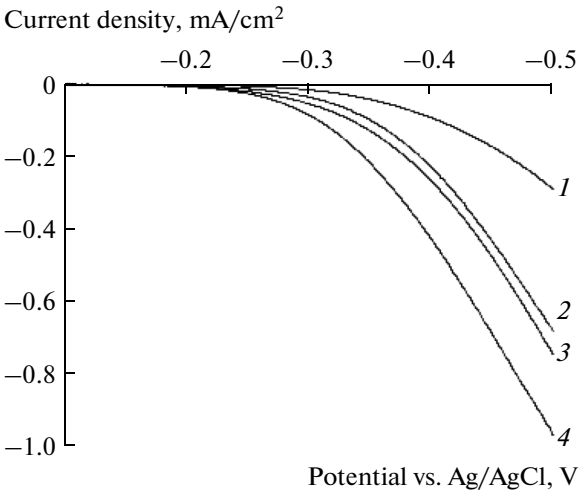

Fig. 9. Current–voltage curves for an electrode made from titanium dioxide in the presence of an $H_3PW_{12}O_{40}$ solution at concentrations of (*1*) 0, (*2*) 5×10^{-5}, (*3*) 5×10^{-4}, and (*4*) 5×10^{-6} mol/L.

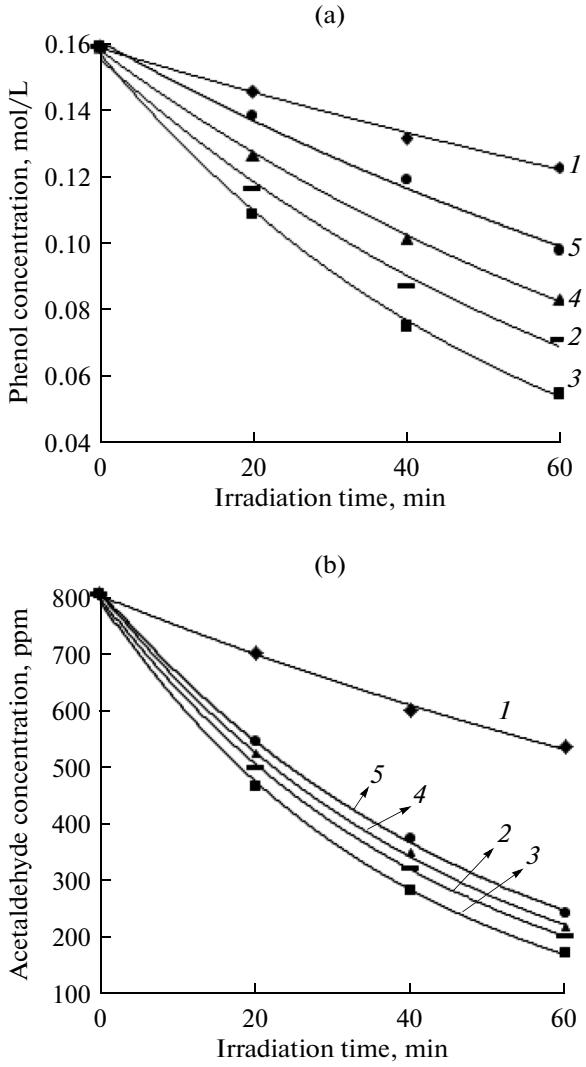

Fig. 10. Kinetics of the decrease of the (a) phenol concentration in aqueous suspension and (b) acetaldehyde concentration in air during the photocatalytic oxidation of the substrates over (*1*) T, (*2*) 0.2P-T, (*3*) 0.5P-T, (*4*) 1.0P-T, and (*5*) 5.0P-T.

Photocatalytic Activity

Photocatalysts containing different amounts of adsorbed $H_3PW_{12}O_{40}$ were tested in reactions of photocatalytic oxidation in aqueous solutions and in the gas phase. Figure 10 illustrates the photooxidation kinetics of dissolved phenol and acetaldehyde vapor. Clearly, the substrate disappearance rate increases as a result of titanium dioxide deposition onto $H_3PW_{12}O_{40}$. In both cases, the highest rate of the photocatalytic reaction was observed with the 0.5P-T sample. The deposition of larger amounts of HPA somewhat reduces the catalytic activity, but it remains well above the activity of the initial titanium dioxide. This is in agreement with the hydroxyl radical generation rate data and interfacial electron transfer data presented in the previous section.

Figure 11 illustrates the time variation of the concentration of phosphate ions resulting from the deep photocatalytic oxidation of triethyl phosphate in aqueous suspensions of photocatalysts containing different amounts of HPA. The formation of phosphate ions confirms the conclusion that triethyl phosphate undergoes total demineralization during photooxidation. The highest phosphate ion formation rate in aqueous solution is again observed for the 0.5P-T sample. Individual titanium dioxide and the 1.0P-T and 5.0P-T samples are less active. For the 0.5P-T and 0.2P-T photocatalysts, the phosphate ion concentration curve flattens out, indicating that triethyl phosphate mineralization is complete.

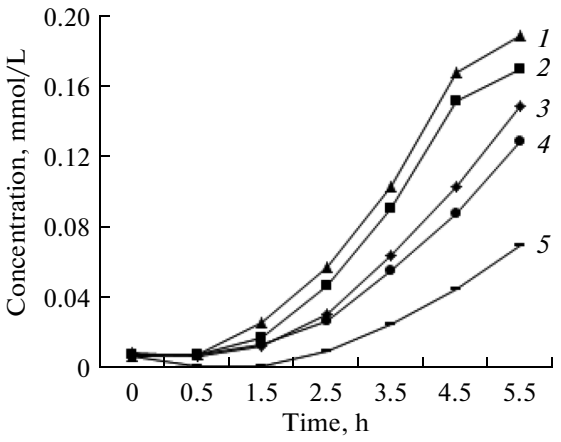

Fig. 11. Kinetics of the variation of the phosphate ion concentration during the photocatalytic oxidation of triethyl phosphate in suspensions of (*1*) 0.5P-T, (*2*) 0.2P-T, (*3*) 1.0P-T, (*4*) 5.0P-T, and (*5*) T.

ACKNOWLEDGMENTS

This study was carried out in the framework of base budgetary financing (project no. V.45.3.2) and was supported in part by the Russian Foundation for Basic Research (project no. 13-08-0128614) and by the Presidium of the Russian Academy of Sciences (project no. 24.49). This study was also supported by a grant from the China Scholarship Council and from the Key NSFC Project (U1401245), the National Key Basic Research Program of China (2014CB660814), the Program for Innovative Research Team in Chinese Universities (IRT1237), and the Research Project of Chinese Ministry of Education (213011A).

REFERENCES

1. Gorokhovskii, A.V., Tret'yachenko, E.V., Vikulova, M.A., Kovaleva, D.S., and Yurkov, G.Yu., *Russ. J. Appl. Chem.*, 2013, vol. 86, no. 3, p. 343.
2. Vinogradov, A.V., Vinogradov, V.V., Ermakova, A.V., and Agafonov, A.V., *Nanotechnol. Russ.,* 2014, vol. 9, p. 15.
3. Obolenskaya, L.N., Dulina, N.A., Savinkina, E.V., and Kuz'micheva, G.M., *Inorg. Mater.,* 2013, vol. 49, no. 6, p. 572.
4. Pugachevskii, M.A., *Nanotechnol. Russ.,* 2013, vol. 8, p. 432.
5. Gavrilov, A.I., Belich, N.A., Shuvaev, S.V., Gil', D.O., Churagulov, B.R., and Gudilin, E.A., *Dokl. Chem.,* 2014, vol. 454, p. 9.
6. Yao, S., Song, S., and Shi, Z., *Russ. J. Phys. Chem. A*, 2014, vol. 88, p. 1066.
7. Zhang, D., *High Energy Chem.*, 2013, vol. 47, p. 177.
8. Zakharenko, V.S. and Daibova, E.B., *High Energy Chem.*, 2014, vol. 48, p. 93.
9. Yao, S., Zhang, Y., Shi, Z., and Wang, S., *Russ. J. Phys. Chem. A*, 2013, vol. 87, p. 69.
10. Fakhrutdinova, E.D., Shabalina, E.D., Mokrousov, G.M., Salanov, A.N., and Wu, J.J., *Russ. J. Inorg. Chem.*, 2014, vol. 59, p. 291.
11. Gavrilov, A.I., Balakhonov, S.V., Gavrilova, D.Yu., Churagulov, B.R., and Gudilin, E.A., *Dokl. Chem,* 2014, vol. 455, p. 58.
12. Rodionov, I.A., Mechtaeva, E.V., and Zvereva, I.A., *Russ. J. Gen. Chem.*, 2014, vol. 84, p. 611.
13. Lv, H., Song, J., Zhu, H., Geletii, Y.V., Bacsa, J., Zhao, C., Lian, T., Musaev, D.G., and Hill, C.L., *J. Catal.,* 2013, vol. 307, p. 48.
14. Zakharova, G.S., Andreikov, E.I., Osipova, V.A., Yatluk, Yu.G., and Puzyrev, I.S., *Inorg. Mater.,* 2013, vol. 49, no. 11, p. 1127.
15. Baklanova, I.V., Krasil'nikov, V.N., Zhukov, V.P., Gyrdasova, O.I., Perelyaeva, L.A., Buldakova, L.Yu., Yanchenko, M.Yu., and Shein, I.R., *Russ. J. Inorg. Chem.*, 2014, vol. 59, p. 29.
16. Zhang, D., *Russ. J. Phys. Chem. A*, 2013, vol. 87, p. 129.
17. Jing, L., Xin, B., Yuan, F., Xue, L., Wang, B., and Fu, H., *J. Phys. Chem. B*, 2006, vol. 110, p. 17860.
18. Cao, Y., Jing, L., Shi, X., Luan, Y., Durrant, J.R., Tang, J., and Fu, H., *Phys. Chem. Chem. Phys.*, 2012, vol. 14, p. 8530.
19. Jing, L., Cao, Y., Cui, H., Durrant, J.R., Tang, J., Liu, D., and Fu, H., *Chem. Commun.,* 2012, vol. 48, p. 10775.
20. Vinogradov, A.V., Vinogradov, V.V., Ermakova, A.V., and Agafonov. A.V, *Nanotechnol. Russ.,* 2013, vol. 8, p. 616.
21. Wang, J., Li, Y., Wang, J., Zhang, L., Gao, J.Q., Wang, B.X., Yang, Q., and Fan, P., *Russ. J. Phys. Chem. A*, 2014, vol. 88, p. 149.
22. He, L., Jing, L., Li, Z., Sun, W., and Liu, C., *RSC Adv.,* 2013, vol. 3, p. 7438.
23. Yang, Y., Liu. e., fan j., hu x., hou w., wu f., ma y, *Russ. J. Phys. Chem. A*, 2014, vol. 88, p. 478.
24. Arkhipova, A.V., Sokolova, T.N., and Kartashov, V.R., *Khim. Rastit. Syr'ya*, 2007, vol. 4, p. 53.
25. Arkhipova, A.V., Malkova, K.V., Sokolova, T.N., and Kartashov, V.R., *Khim. Rastit. Syr'ya*, 2006, vol. 4, p. 11.
26. Damyanova, S., Cubeiro, M.L., and Fierro, J.L.G., *J. Mol. Catal. A: Chem.*, 1999, vol. 142, p. 85.
27. Liu, B., Yang, J., Yang, G.-C., and Ma, J.-F., *Inorg. Chem.,* 2013, vol. 52, p. 84.
28. Guo, Y., Wang, Y., Hu, C., Wang, Y., Wang, E., Zhou, Y., and Feng, S., *Chem. Mater.,* 2000, vol. 12, p. 3501.
29. Hu, C., Yue, B., and Yamase, T., *Appl. Catal., A*, 2000, vol. 194, p. 99.
30. Moriguchi, I., Orishikida, K., Tokuyama, Y., Watabe, H., Kagawa, S., and Teraoka, Y., *Chem. Mater.,* 2001, vol. 13, p. 2430.
31. Li, M., Xu, C., Ren, J., Wang, E., and Qu, X., *Chem. Commun.,* 2013, vol. 49, p. 11394.
32. Hori, H., Yamamoto, A., Koike, K., Kutsuna, S., Murayama, M., Yoshimoto, A., and Arakawa, R., *Appl. Catal., B*, 2008, vol. 82, p. 58.

33. Antonaraki, S., Androulaki, E., Dimotikali, D., Hiskia, A., and Papaconstantinou, E., *J. Photochem. Photobiol., A*, 2002, vol. 148, p. 191.

34. Friesen, D.A., Headley, J.V., and Langford, C.H., *Environ. Sci. Technol.*, 1999, vol. 33, p. 3193.

35. Halimehjani, A.Z., Farvardin, M.V., Zanussi, H.P., Ranjbari, M.A., and Fattahi, M., *J. Mol. Catal. A: Chem.*, 2014, vol. 381, p. 21.

36. Thanasilp, S., Schwank, J.W., Meeyoo, V., Pengpanich, S., and Hunsom, M., *J. Mol. Catal. A: Chem.*, 2013, vol. 380, p. 49.

37. Qiao, Y., Hua, L., Chen, J., Theyssen, N., Leitner, W., and Hou, Z., *J. Mol. Catal. A: Chem.*, 2013, vol. 380, p. 43.

38. Yoon, M., Chang, J.A., Kim, Y., Choi, J.R., Kim, K., and Lee, S.J., *J. Phys. Chem. B,* 2001, vol. 105, p. 2539.

39. Li, J., Kang, W., Yang, X., Yu, X., Xu, L., Guo, Y., Fang, H., and Zhang, S., *Desalination,* 2010, vol. 255, p. 107.

40. Cai, T., Liao, Y., Peng, Z., Long, Y., Wei, Z., and Deng, Q., *J. Environ. Sci.*, 2009, vol. 21, p. 997.

41. Wang, S.-M., Liu, L., Chen, W.-L., Su, Z.-M., Wang, E.-B., and Li, C., *Ind. Eng. Chem. Res.*, 2014, vol. 53, p. 150.

42. Pruethiarenun, K., Isobe, T., Matsushita, S., and Nakajima, A., *Appl. Catal., A,* 2012, vols. 445–446, p. 274.

43. Li, D., Guo, Y., Hu, C., Jiang, C., and Wang, E., *J. Mol. Catal. A: Chem.,* 2004, vol. 207, p. 183.

44. Zhang, X., Lei, L., Zhang, J., Chen, Q., Bao, J., and Fang, B., *Sep. Purif. Technol.*, 2009, vol. 67, p. 50.

45. Liu, C., Jing, L., He, L., Luan, Y., and Li, C., *Chem. Commun.,* 2014, vol. 50, p. 1999.

46. Zhang, S., Chen, L., Liu, H., Guo, W., Yang, Y., Guo, Y., and Huo, M., *Chem. Eng. J.*, 2012, vols. 200–202, p. 300.

47. Ma, Y., Liu, Y., Xiao, X., Li, X., and Zhou, X., *Chin. Sci. Bull.*, 2005, vol. 50, p. 1985.

48. Lin, F., Cheng, J., Engtrakul, C., Dillon, A.C., Nordlund, D., Moore, R.G., Weng, T.-C., Williams, S.K.R., and Richards, R.M., *J. Mater. Chem.*, 2012, vol. 22, p. 16817.

Translated by D. Zvukov